Computer Standards & Interfaces 50 (2017) 18–25

Contents lists available at ScienceDirect

Computer Standards & Interfaces

journal homepage: www.elsevier.com/locate/csi

A new full-reference image quality metric based on just noticeable difference

Sevil Toprak, Yildiray Yalman*

Department of Computer Engineering, Turgut Ozal University, Ankara, Turkey

ARTICLE INFO

Keywords:
Image quality metric
Full-reference image quality metric
Human vision system
Just noticeable difference

ABSTRACT

An Image Quality Metric (IQM) is used to measure how the image on which modifications are carried out is distorted. Knowing the distortion scale of the image is of significance for the intended purposes (compression, forensic, medical, etc.). The amount of distortion has different implications for each of the application and whether the image is convenient for the relevant application by using the IQM. One of the most basic approaches in the literature which is used in measuring the amount of the distortion is the Full-Reference Image Quality Metric (FR-IQM). The FR-IQM needs both the original and distorted image in the phase of comparison. In this study, taking into consideration the Human Vision System (HVS), a new full-reference image quality metric based on Just Noticeable Difference (JND) has been presented. Through this new metric, the HVS's physiological (color and light sensitivity) and psycho-physiological (texture and edge sensitivity) characteristics have been taken into consideration. Through the JND, the inclusion of the unintended modifications that cannot be sensed by the HVS has been prevented. The near-zero quality results point out the more quality image. The experimental results have showed that the metric in question demonstrates a higher level of performance for the HVS when compared with its counterparts.

1. Introduction

Most of the time, the obtained digital images are either coded or they are subjected to modifications for different purposes. The Image Quality Metric is used when one wishes to know how these modifications distort the image. While determining the level of distortion of the image, it is of paramount importance to take into consideration such questions as to whom/to what/for what purpose. An image can be solely used at visual examination and it can also be used for the medical diagnosis or various analysis. The level of distortion of the image has different implications for each one of the applications and it determines whether the image is usable for the relevant application. For this reason, the “application-specific” image quality measurement methods are of great significance [1].

The IQMs in the literature are separated into 3 groups: full-reference IQM [2], reduced-reference IQM [3] and no-reference IQM [4]. The Full-reference IQM need both the distorted and original image. By taking the original image as a reference, how different the distorted image is calculated. However, there is not reference image as regards the no-reference IQM. For this reason, while comparing, only one image is taken into consideration. In the reduced-reference IQMs which can be considered to be a method between these two methods, the quality of the distorted image is measured by partially using the reference image [5–7].

There are still serious shortcomings regarding the development of algorithms which take into account all characteristics of the HVS, which are robust, practical and adequately respond to the needs. In the IQM methods in the literature, it has been found that;

(a) Results have been produced for the modifications not perceived by the HSV.
(b) The physiological characteristics of the HVS are not fully taken into consideration.
(c) The HVS's sensitivity to the luminance, texture and edge (psycho-physiological characteristics) are not taken into consideration.
(d) Even though the color and luminance information is paramount importance for the HVS (physiological properties), the quality measurement procedures are carried out after the conversion of the images into the grayscale image [7–12].

The basic objective in this paper is to develop a new quality metric based on the HVS for the digital images and obtain a metric producing the numeric quality results compatible with the HVS by taking the image as a whole.

* Corresponding author.
E-mail address: yildiray.yalman@gmail.com (Y. Yalman).

http://dx.doi.org/10.1016/j.csi.2016.08.003
Received 6 June 2016; Received in revised form 15 July 2016; Accepted 7 August 2016
Available online 13 September 2016

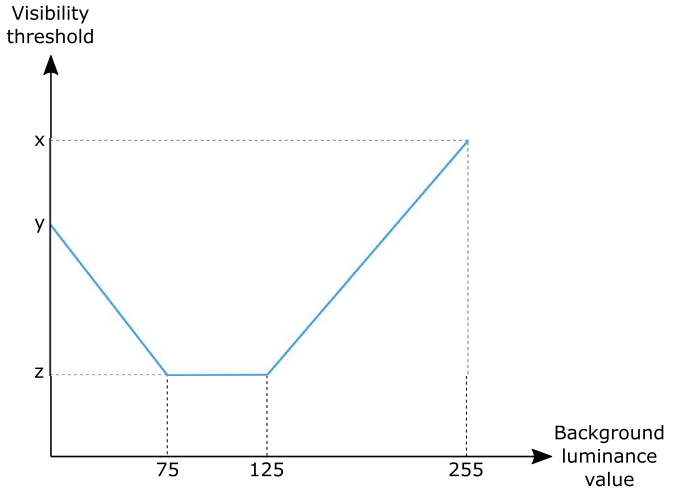

Fig. 1. Visibility threshold according to the amount of background luminance [14,17].

With the metric presented, it has been aimed at eliminating the aforementioned shortcomings and obtaining results compatible with the HVS. Similarly, a method [13] presented for JPEG compressed images in the literature. This means that the method can only measure JPEG compression distortions (i.e., blocking effect). On the contrary, not only JPEG compression but also some other noise types (Gaussian, salt and pepper, speckle, etc.) can easily measure in the presented method. Additionally the presented method takes into account texture information on images (original and distorted) and the number of sensor cells (rods and cones) in the human eye. Therefore, more suitable metric has been presented for the HVS.

In Section 2, the motivation of the proposed method and basic knowledge have been provided and details regarding the metric presented in Section 3 have been given. Experimental results and discussions have been given in Section 4. Final remarks have been presented in Section 5.

2. Basic knowledge

2.1. Peak signal noise ratio (PSNR)

The PSNR is one of the FR-IQMs and it is widely used in the literature. While calculating the result of the PSNR, first of all, the Mean Square Error (MSE) is calculated between the original (O) and distorted (D) images (Eq. (1)). Afterwards, Eq. (2) is used and the final quality result (PSNR) is obtained [14]. When the equations are examined, it will be found that the characteristics of the HVS are not taken into consideration while the PSNR value is calculated:

$$MSE = \frac{1}{M}\left(\sum_{i=1}^{M}(O_i - D_i)^2\right) \tag{1}$$

$$PSNR = 10\log\left(\frac{255^2}{MSE}\right) \tag{2}$$

2.2. YUV transformation

The HVS's sensitivity to the color and light is different. For this reason, RGB–YUV transformation is applied in order to separate the color and light knowledge of the image. The irreversible YUV transformation used in the study has been demonstrated in Eq. (3) [8,15]. After the use of this equation, while Y channel of the YUV image provides light (black–white) knowledge, U (blue) and V (red) channels provide color knowledge:

$$Y = 0.257R + 0.504G + 0.098B + 16U = -0.148R - 0.291G + 0.439B + 128V = 0.439R - 0.368G - 0.071B + 128 \tag{3}$$

2.3. Just noticeable difference (JND)

JND is used for the detection of the locations of the modifications between the pixel values of the both (original and distorted) images that can be discerned through the HVS (Fig. 1) [14,16–19]. Thus, with the help of a threshold (x, y, z), the modifications that cannot be perceived by the HVS are not included. Details about x, y and z values have been given in Section 3.2, Phase 2. JND is used in order to ensure these calculations are not included into these values.

2.4. The structure of the human eye

The structure of the human eye is shown in Fig. 2. In order for the human eyes to see, one of the most basic requirements is the sensory of the light and color. The retina shown in the figure has rod (120 million) and cone cells (7 million). Of these two types of sensors that are spread all across the retina, rod cells are sensitive solely to the light and cone cells solely to colors. While the rate of the rod sensors spread all across the retina in terms of the total number of sensors is approximately

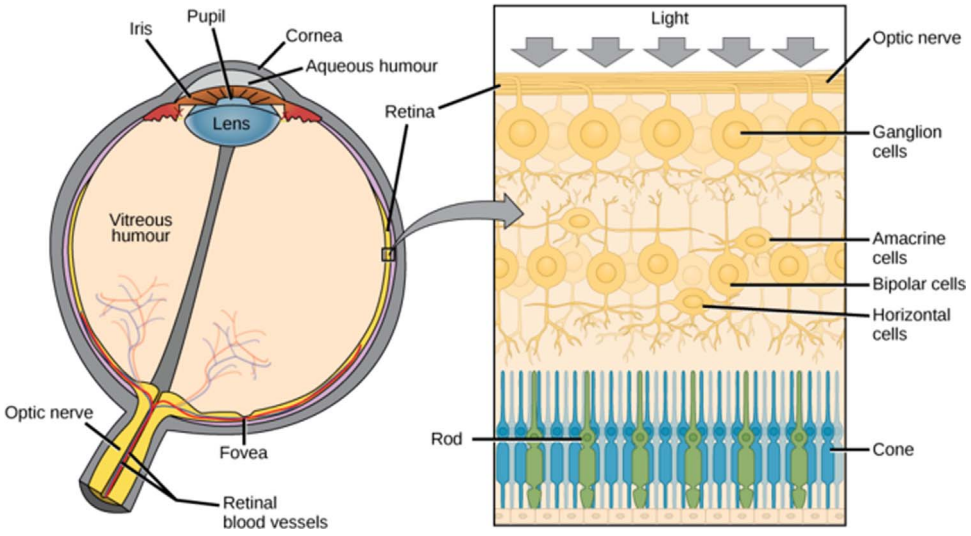

Fig. 2. The structure of the human eye and rod–cone cells [20].

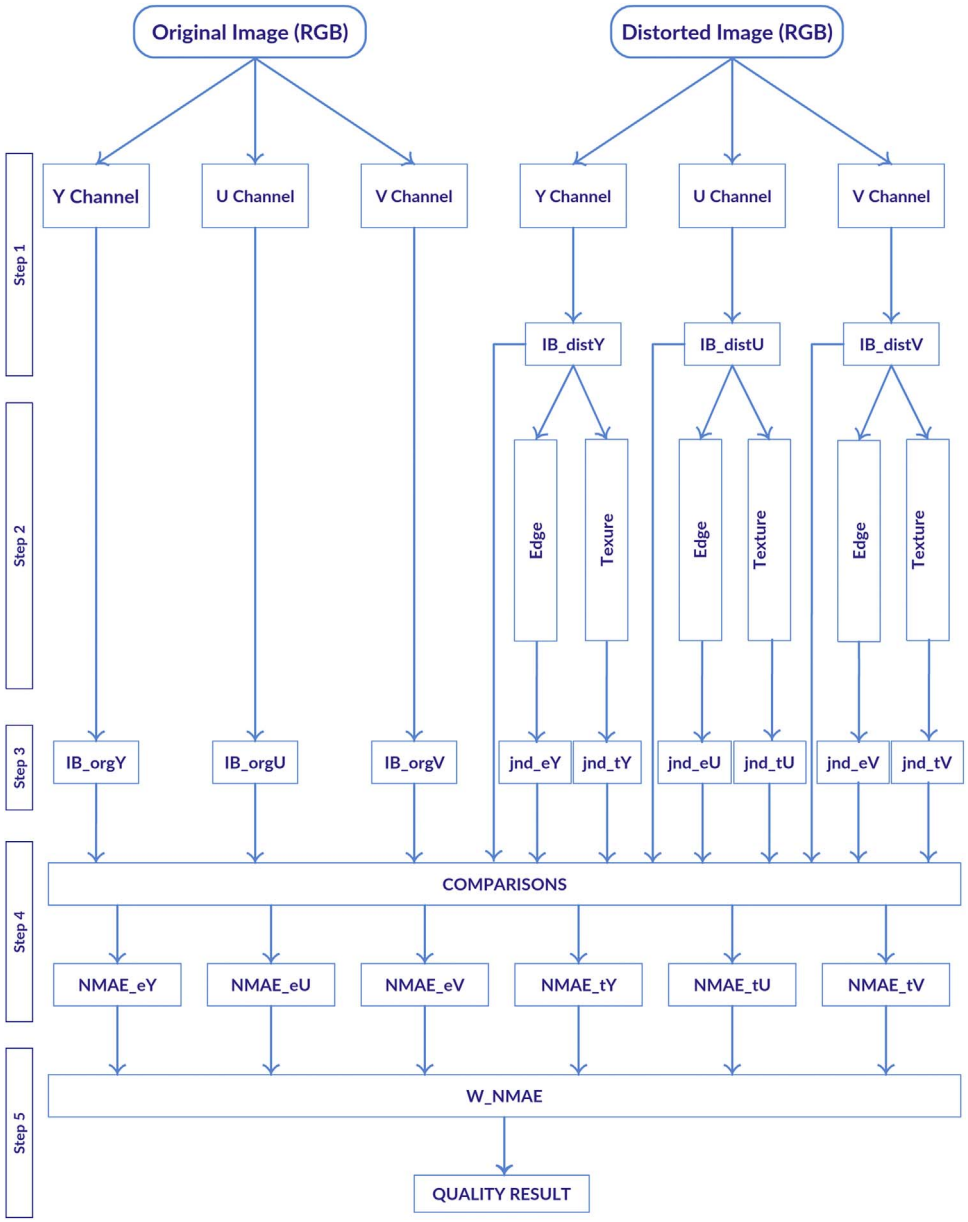

Fig. 3. The general scheme of the proposed method.

95%, this rate is 5% for the cone sensors. The conclusion that can be derived from these rates is that the HVS is more sensitive to the light [1,8].

3. The proposed full-reference IQM: weighted noticeable mean absolute error

The proposed IQM consists of a total of 5 steps. In these steps, the procedures are carried out by taking the HVS as the basis. They are demonstrated in Fig. 3 and they have been defined below as sub-headings. When one wishes to develop a HVS-based quality metric, it is possible to eliminate the above-mentioned literature shortcomings in accordance with the following provisions:

(a) The HVS's sensitivity to light and color is different [21]. This difference can be taken into consideration with the RGB–YUV transformation of the images (original and distorted images) (Step 1).
(b) If the modification of the value anywhere throughout the channel of the obtained YUV images is above the JND [17–19] threshold, it must be taken into consideration and thus, sensory threshold of the HVS will have been taken into consideration (Step 2).
(c) The texture and edge knowledge of crucial significance in terms of the psycho-physiological characteristics of each channel of the YUV images must be detected through the appropriate filters (Steps 3 and 4).
(d) The value obtained as a result of these steps must be weighted taking into consideration the physical characteristics of the HVS (the number of the rod and cone cells in the eye). As a result of these steps, the quality result will have been obtained by taking into consideration the HVS's physiological and psycho-physiological characteristics and light and color knowledge on the colorful digital images (Step 5).

3.1. Step-1

By using Eq. (3), the YUV transformation is applied to the original and distorted RGB images to be compared. Y, U and V channels

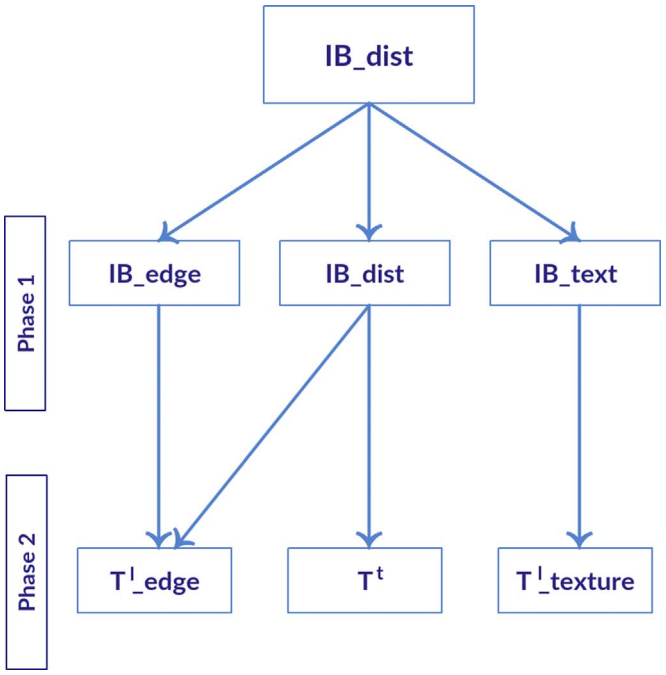

Fig. 4. Texture and edge calculations for Step 2.

pertaining to the original and distorted images following the YUV transformation are obtained. Each of the Y, U, V channels of the distorted image is separated into 7×7 image blocks (IB) and Step 2, Step 3 and Step 4 are applied to each block.

3.2. Step-2

With the help of the IBs for distorted image (*IBdist*) obtained after the Step 1 for each YUV channel (*IBdistY*, *IBdistU*, *IBdistV*), JND threshold value is determined by using edge and texture knowledge of great importance in terms of the HVS's psycho-physiological characteristics. The procedures carried out in this step are shown in detail in Fig. 4. Its details have been provided below:

- *Phase* 1: The edge and texture knowledge (*IBedge*, *IBtext*) is found for each channel (Y, U, V). Sobel filter has been used for edge detection on the original and distorted images. It is widely used in image processing operations, particularly within edge detection algorithms. When this filter is used, the operator uses two 3×3 image blocks which are convolved with the original image to calculate approximations of the derivatives one for horizontal changes, and another one for vertical. If the source image is as I, and G_x and G_y are two images which at each point contain the horizontal and vertical derivative approximations respectively, the calculations can be realized as follows:

$$G_x = \begin{bmatrix} -1 & 0 & +1 \\ -2 & 0 & +2 \\ -1 & 0 & +1 \end{bmatrix} * I \tag{4}$$

$$G_y = \begin{bmatrix} -1 & -2 & -1 \\ 0 & 0 & 0 \\ +1 & +2 & +1 \end{bmatrix} * I \tag{5}$$

where * here denotes the 2-dimensional signal processing convolution operation [22].

Since the Sobel kernels can be decomposed as the products of an averaging and a differentiation kernel, they compute the gradient with smoothing. The x-coordinate is defined here as increasing in the "right"-direction, and the y-coordinate is defined as increasing in the "down"-direction. At each point in the image, the resulting gradient approximations can be combined to give the gradient magnitude, using:

$$G = \sqrt{G_x^2 + G_y^2} \tag{6}$$

In order to obtain the texture knowledge, the *rangefilt*() function in the MATLAB platform has been used [23]. *rangefilt*() function calculates the local range of an image as seen in Fig. 5.

- *Phase* 2: In Eq. (7), the background luminance value (T^l) is calculated. This value is one of the variables used in the calculation of the JND value. The values of the parameters used in order to find the background luminance value is taken as x=24, y=20 and z=10 ($T^l texture$). These values are taken as x=22, y=18 and z=8 ($T^l edge$) if there is an edge detection in calculated IB [14,24]. Another variable used in the calculation of the JND value is the visibility threshold (T^t) and it is calculated through the formula shown in Eq. (8). These steps are renewed for each channel (*IBdistY*, *IBdistU*, *IBdistV*).

$$T^l = \begin{cases} y - \dfrac{y - z}{75}\overline{D(i,j)}, & \overline{D(i,j)} \le 75 \\ \dfrac{x - z}{130}\overline{D(i,j)} + \dfrac{255}{130}z - \dfrac{125}{130}x, & \overline{D(i,j)} \ge 125 \\ z, & \text{otherwise} \end{cases} \tag{7}$$

$$T^t = \max(\overline{D(i,j)}) - \min(\overline{D(i,j)}) \tag{8}$$

3.3. Step-3

By using T^t, T^l_edge and T^l_texture values obtained in the previous step, JND threshold values (*jnde*, *jndt*) are calculated for edge and texture version of the distorted image (Eq. (9)). These calculations are renewed for each channel (Y, U, V). β value in this formula is taken as 0.5 [14]:

$$JND = T^l + \frac{\beta * T^t}{T^l} \tag{9}$$

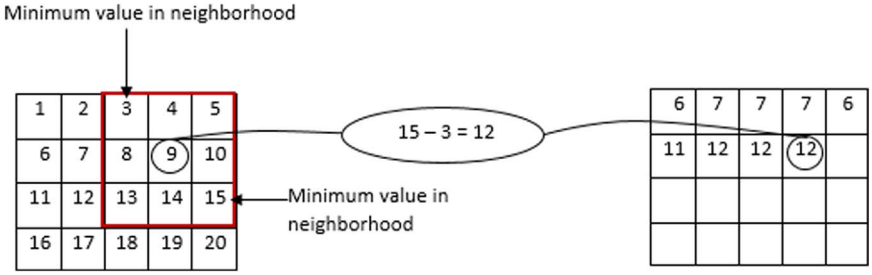

Fig. 5. Description of rangefilt() function.

(a) Original Image (b) Gaussian

(c) Salt and pepper (d) Sharpen

(e) Median (f) Blurring

Fig. 6. Test Images – Lena (a) and its distorted versions (b)–(f).

Table 1
Results of FR-IQMs for Lena (a) and its different distorted versions (b)–(f).

Images	*PSNR* (dB)	*SSIM*	*UQI*	*VIF*	*WNMAE*
Fig. 6(b)	27.6707	0.6285	0.5258	0.8590	0.0252
Fig. 6(c)	27.6707	0.8641	0.8204	0.8692	0.0313
Fig. 6(d)	27.6707	0.9098	0.8699	0.9886	0.0510
Fig. 6(e)	27.6707	0.7683	0.4989	0.7584	0.1045
Fig. 6(f)	27.6707	0.7830	0.6147	0.7035	0.1548

3.4. Step-4

In this step, the original and distorted image blocks (*IBorg*, *IBdist*) are compared. While carrying out this comparison, the JND values (*jnde*, *jndt*) obtained in Step 3 for each channel are taken into consideration (Eq. (10)). These calculations are carried out for each color channel (Y, U, V). Error amount (*NMAEeY*, *NMAEeU*, *NMAEeV*, *NMAEtY*, *NMAEtU*, *NMAEtV*) called the Noticeable Mean Absolute Error (NMAE) are detected for each color channel by using Eq. (11) (*NMAEeY* means that NMAE calculation on Y channel for edge version of the distorted image).

(a) Original Image (b) Smart Sharpen

(c) Sharpen and Unsharp Masking (d) More Sharpen and Smart Sharpen

(e) Speckle Noise (f) Gaussian Blur

Fig. 7. Test Images – Original Image (a) and its distorted versions (b)–(f).

Table 2
Results of FR-IQMs for the original image (a) and its different distorted versions (b)–(f).

Images	*PSNR* (dB)	*SSIM*	*UQI*	*VIF*	*WNMAE*
Fig. 7(b)	28.337	0.9140	0.7207	0.8385	0.0607
Fig. 7(c)	28.337	0.9299	0.8744	0.9661	0.0778
Fig. 7(d)	28.337	0.9130	0.8384	0.9342	0.0851
Fig. 7(e)	28.337	0.8525	0.6206	0.9366	0.1183
Fig. 7(f)	28.337	0.8748	0.7061	0.9472	0.1333

$$d(i,j) = \begin{cases} 0, & |O(i,j) - D(i,j) \le JND| \\ \left| \dfrac{O(i,j) - D(i,j)}{JND} \right|, & \text{otherwise} \end{cases} \tag{10}$$

$$NMAE = \frac{1}{7 \times 7}\left(\sum_{i=1}^{7} \sum_{j=1}^{7} (d(i,j)) \right) \tag{11}$$

3.5. Step-5

NMAE values obtained in the previous step are used and Weighted Noticeable Mean Absolute Error (WNMAE) is calculated by taking into consideration the distribution pertaining to the rod–cone cells all across the retina (Eq. (12)). Therefore, the density of the rod and cone cells on the HVS is taken into consideration in the calculation. Thus quality impact of the Y channel is weighted as 95% and U and V channels are weighted as 5%. The best result of the WNMAE value to be obtained is 0. This means that the near zero WNMAE quality results points out the more quality image.

$$\begin{aligned} WNMAE = {} & ((NMAE_eY + NMAE_tY)/2).\ 0.95 \\ & + ((NMAE_eU + NMAE_eV + NMAE_tU + NMAE_tV)/4).\ 0.05 \end{aligned} \tag{12}$$

Easy MATLAB implementation of the proposed metric can be downloaded from http://bit.ly/1TYJYn5.

4. Experimental results

The steps described in Section 3 have been applied to the various image groups and the results obtained have been presented below. It

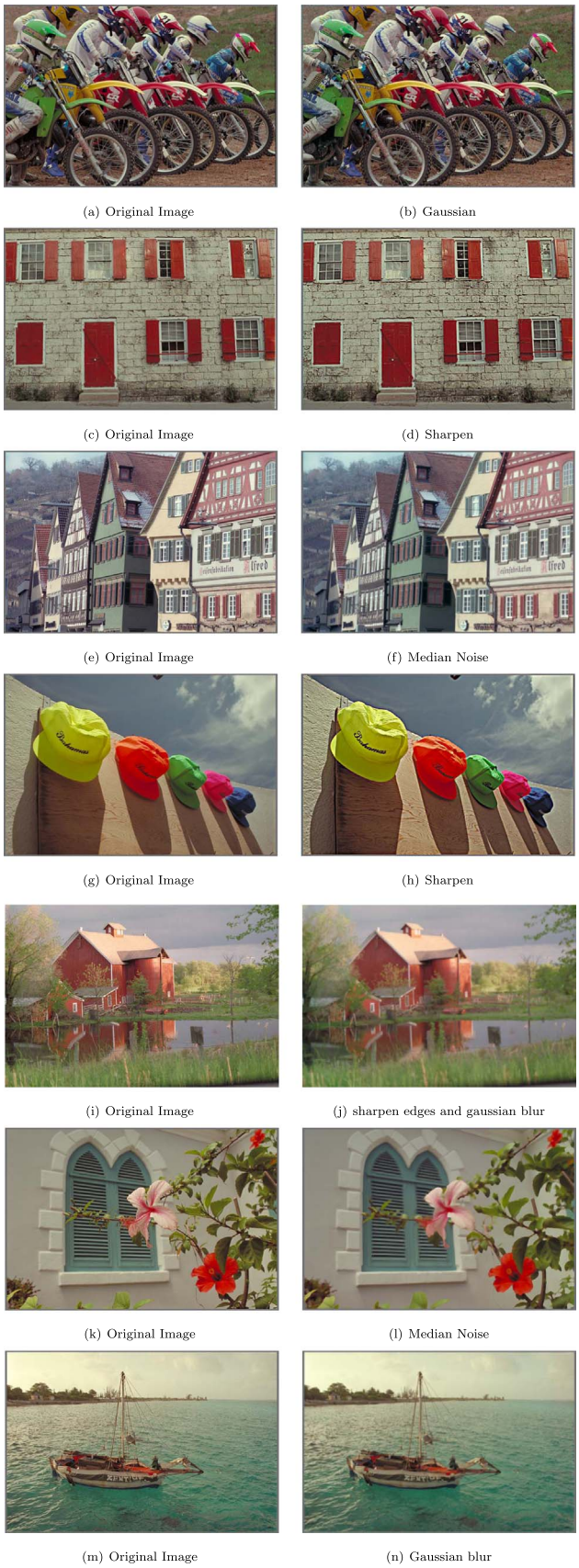

(a) Original Image (b) Gaussian

(c) Original Image (d) Sharpen

(e) Original Image (f) Median Noise

(g) Original Image (h) Sharpen

(i) Original Image (j) sharpen edges and gaussian blur

(k) Original Image (l) Median Noise

(m) Original Image (n) Gaussian blur

Fig. 8. Different original images and their distorted versions.

Table 3
Results of FR-IQMs for the different original images and its different distorted versions.

Images	*PSNR* (dB)	*SSIM*	*UQI*	*VIF*	*WNMAE*
Fig. 8(a) and (b)	28.0555	0.8594	0.8699	0.8842	0.0082
Fig. 8(c) and (d)	28.0555	0.9442	0.9343	0.9389	0.0877
Fig. 8(e) and (f)	28.0555	0.9324	0.9184	0.9730	0.0999
Fig. 8(g) and (h)	28.0555	0.9070	0.8174	0.8021	0.1024
Fig. 8(i) and (j)	28.0555	0.7808	0.6691	0.8886	0.1158
Fig. 8(k) and (l)	28.0555	0.8930	0.7350	0.8092	0.1218
Fig. 8(m) and (n)	28.0555	0.8273	0.7513	0.9450	0.1347

has been found that the WNMAE values pertaining to the images used within this scope have provided compatible results with the HVS. We consider some high impacted IQMs presented in the literature for experimental studies. The quality values being near 1 for all Structural Similarity (SSIM) [7], Universal Quality Index (UQI) [9] and Visual Information Fidelity (VIF) [25] metrics mean that the calculated image is better quality. The WNMAE quality results obtained for the distorted images given in Fig. 6 are presented in Table 1.

The accurate order from the best to the worst of the distorted versions of the Lena image according to the WNMAE is shown in Fig. 6(b)–(f). As can be seen in Table 1, all the relevant images have the same PSNR value. While Fig. 6(f) was anticipated to have the worst quality value in terms of the HVS, Fig. 6(b) is the worst image for the SSIM and Fig. 6(e) is the worst one for the UQI. Likewise, according to the VIF, Fig. 6(d) is the image with the least distortion. However, when we take the HVS into consideration, the sharpen effect in Fig. 6(d) is clearly seen. These results show that the distortion or modification amount on the images is found to be compatible with the HVS as the WNMAE takes into consideration the HVS.

Likewise, when the WNMAE metric is used to measure the quality of the images in Fig. 7, the results in Table 2 have been obtained.

While Fig. 7(f) was anticipated to have the worst value in terms of the HVS, according to the SSIM and the UQI, Fig. 7(e) is the worst image. Likewise, according to the VIF, Fig. 7(f) is better than Fig. 7(b), (d), (e). This shows that the relevant metrics do not provide results compatible with the HVS. On the contrary; the WNMAE results more compatible than its counterparts.

Finally the presented metric and other quality metrics are used for the images presented in Fig. 8, the results in Table 3 have been obtained. Here, a 7-different-image group consisting of an original image and its distorted version is used. While comparing these images, one must take into consideration how different the distorted version is from the original one. As can be seen, the PSNR produces the same quality result for each distorted image. Even though the other metrics produce different results, as in the other applications, they do not produce results compatible with the HVS. It has been found that the WNMAE has produced better results compatible with the HVS than its counterparts.

The results obtained in the table have been got through the application of the PSNR, the SSIM, the UQI, the VIF and the WNMAE to each image. When the results of these metrics are analyzed, it can be easily seen that the best metric producing results compatible with the HVS is the WNMAE. Taking into consideration the HVS's characteristics play an important role in good results produced by the method of the WNMAE. However, as the sensory of individuals vary, the order may not be the same for anybody. That said, while the PSNR produces the same values for all the images, the WNMAE produces different and compatible results with the HVS for these images.

5. Conclusions

The level of distortion on an image means different implications for different purposes and determines whether the image is usable for the application. For this reason, the use of appropriate image quality

measurement methods is of great importance. In this paper, a new IQM based on the JND taking into consideration the HVS's characteristics has been presented.

Being different from the similar methods in the literature, this method produces quality results by taking into consideration the HVS's physiological (number of cells rod and cone cells on the eye) and psychophysiological (texture and edge knowledge) characteristics. While producing the relevant result, the JND which plays a central role in the determination of the sensory threshold is used. Thus, the distortions under the visual sensory threshold are not taken into consideration in the calculations.

It has been found that the nearer the produced quality result to the value of 0, the more quality (less distorted) the distorted image measured. The experimental results obtained demonstrate that the presented method produces more compatible results with the HVS in comparison with such quality metrics as the PSNR, the MSSIM, the VIF which are widely used by the researchers as the quality metrics.

Acknowledgments

This work has been supported in part by The Scientific and Technological Research Council of Turkey (TUBITAK) research grant 115E651. The authors would like to thank the anonymous reviewers and the editor for their invaluable comments and suggestions.

References

[1] Y. Yalman, Histogram based perceptual quality assessment method for color images, Comput. Stand. Interfaces 36 (6) (2014) 899–908.
[2] E.C. Larson, D.M. Chandler, Most apparent distortion: full-reference image quality assessment and the role of strategy, J. Electron. Imaging 19 (1) (2010) 1–21.
[3] D. Liu, Y. Xu, Y. Quan, P.L. Callet, Reduced reference image quality assessment using regularity of phase congruency, Signal Process.: Image Commun. 29 (8) (2014) 844–855.
[4] H.R. Sheikh, A.C. Bovik, L. Cormack, No-reference quality assessment using natural scene statistics: jpeg2000, IEEE Trans. Image Process. 14 (11) (2005) 1918–1927.
[5] F. Gao, J. Yu, Biologically inspired image quality assessment, Signal Process. 124 (2016) 210–219.
[6] L. He, D. Tao, X. Li, X. Gao, Sparse representation for blind image quality assessment, in: IEEE Conference on Computer Vision and Pattern Recognition (CVPR), 2012, pp. 1146–1153.
[7] Z. Wang, A.C. Bovik, H.R. Sheikh, E.P. Simoncelli, Image quality assessment: from error visibility to structural similarity, IEEE Trans. Image Process. 13 (4) (2004) 600–612.
[8] Y. Yalman, I. Erturk, A new color image quality measure based on yuv transformation and psnr for human vision system, Turk. J. Electr. Eng. Comput. Sci. 21 (2) (2013) 312–603.
[9] Z. Wang, A.C. Bovik, A universal image quality index, IEEE Signal Process. Lett. 9 (3) (2002) 81–84.
[10] Z. Wang, E.P. Simoncelli, A.C. Bovik, Multi-scale structural similarity for image quality assessment, Signals Syst. Comput. 2 (2003) 1398–1402.
[11] H.R. Sheikh, A.C. Bovik, Image information and visual quality, IEEE Trans. Image Process. 15 (2) (2006) 430–444.
[12] K. Egiazarian, J. Astola, N. Ponomarenko, V. Lukin, F. Battisti, M. Carli, New full-reference quality metrics based on hvs, in: 2nd International Workshop on Video Processing and Quality Metrics: VPQM06, USA.
[13] S. Suthaharan, S.W. Kim, K.R. Rao, A new quality metric based on just-noticeable difference, perceptual regions, edge extraction and human vision, Can. J. Electr. Comput. Eng. 30 (2) (2005) 81–88.
[14] W. Lin, L. Dong, P. Xue, Visual distortion gauge based on discrimination of noticeable contrast changes, IEEE Trans. Circuits Syst. Video Technol. 15 (7) (2005) 900–909.
[15] Y. Chen, P. Hao, Integer reversible transformation to make jpeg lossless, in: IEEE International Conference on Signal Processing, vol. 1, 2004, pp. 835–838.
[16] S. Schwartz, Visual Perception: A Clinical Orientation, fourth ed. ISBN: 978-0-07-160462-8, 2010
[17] C. Chou, Y. Li, A perceptually tuned subband image coder based on the measure of just-noticeable-distortion profile, IEEE Trans. Circuits Syst. Video Technol. 5 (6) (1995) 467–476.
[18] R. Legras, N. Chateau, W.N. Charman, Assessment of just-noticeable differences for refractive errors and spherical aberration using visual simulation, Optom. Vis. Sci. 81 (9) (2004) 718–728.
[19] Y. Niu, J. Liu, S. Krishnan, Q. Zang, Combined just noticeable difference model guided image watermarking, in: IEEE International Conference on Multimedia and Expo, 2010, pp. 1679–1684.
[20] Anatomy of the eye, ⟨https://www.boundless.com/biology/textbooks/boundless-biology-textbook/sensory-systems-36/vision-209/anatomy-of-the-eye-789-12024/⟩, 2016 (accessed 01.06.16).
[21] H. Qi, D. Zheng, J. Zhao, Human visual system based adaptive digital image watermarking, Signal Process. 88 (1) (2008) 174–188.
[22] W. Yang, X. Wang, B. Moran, A. Wheaton, N. Cooley, Efficient registration of optical and infrared images via modified Sobel edging for plant canopy temperature estimation, Comput. Electr. Eng. 38 (5) (2012) 1213–1221.
[23] Texture analysis, ⟨http://www.mathworks.com/help/images/texture-analysis.html⟩, 2016 (accessed 01.06.16).
[24] S.W. Jung, L.T. Ha, S.J. Ko, A new histogram modification based reversible data hiding algorithm considering the human visual system, IEEE Signal Process. Lett. 18 (2) (2011) 95–98.
[25] Y. Han, Y. Cai, Y. Cao, X. Xu, A new image fusion performance metric based on visual information fidelity, Inf. Fusion 14 (2) (2013) 127–135.